Keehm, Y., Mukerji, M., Nur, A., Computational rock physics: Lattice-Boltzmann fluid flow simulation in porous media and its applications.
International Symposium on the Fusion Technology of Geosystem Engineering, Rock Engineering and Geophysical Exploration
Seoul, Korea, Nov. 18-19, 2003

Computational rock physics: Lattice-Boltzmann fluid flow simulation in porous media and its applications

Youngseuk Keehm, Tapan Mukerji, Amos Nur
Stanford University, Stanford, CA 94305, USA

Abstract: This paper presents Lattice-Boltzmann simulation techniques for single-phase and two-phase fluid flow in porous media. Numerical experiments were performed in a digital rock sample from X-ray microtomography. Computed results showed very good agreement with laboratory measurements of permeability and relative permeability. Two applications using these simulation techniques show the potential of the Lattice-Boltzmann flow simulation to solve many difficult problems coupled with fluid flow in porous media.

1. Introduction

Earth sciences is undergoing a gradual but massive shift from description of the earth and earth systems, toward process modeling, simulation, and process visualization. This shift is very challenging because the underlying physical and chemical processes are often nonlinear and coupled. In addition, we are especially challenged when the processes take place in strongly heterogeneous systems. An example is two-phase fluid flow in rocks, which is a nonlinear, coupled and time-dependent problem and occurs in complex porous media. To understand and simulate these complex processes, the knowledge of underlying pore-scale processes is essential. A rigorous pore-scale simulator requires three important traits: reliability, efficiency, and ability to handle complex microstructures. We implemented single-phase and two-phase flow simulators using the Lattice-Boltzmann algorithm, since it handles very complex pore geometries rigorously and predict flow properties accurately. In the following chapters, we will cover implementations and results on single-phase and two-phase flow simulations, and two applications using the implementations.

2. Single-phase Lattice-Boltzmann Flow Simulation

The Lattice-Boltzmann (LB) method is based on cellular automata theory, which describes a complex system by the interaction of a massive number of particles following simple local rules (Doolen, 1990; Chen et al., 1992; Chopard and Droz, 1998). Although the particles have nearly nothing in common with real fluids, the rules in the Lattice-Boltzmann method recover the Navier-Stokes equations at the macroscopic scale (Ladd, 1994; Rothman and Zaleski, 1997). While other methods, such as network models, the FEM or the FDM, discretize the model and the governing equations, the LB method recovers the governing equation (Navier-Stokes equations) from rules in the discrete model. This gives the biggest advantage of the Lattice-Boltzmann method that it is readily applied to any arbitrary discrete geometry (Ladd, 1994; Martys and Chen, 1996; Keehm et al., 2001). In addition, it describes fluid flow in porous media very accurately. This strength comes from the characteristics of the LB algorithm. Although the LB method uses a regular Cartesian grid like the FDM, one node has 18 different velocity directions in 3D. This high angular coverage can give an accurate boundary condition on the pore-grain boundaries, equivalent to the one by the FEM with extensive meshing. In essence, the LBM can simulate fluid flow with the high accuracy of the FEM but with the simplicity of the FDM (Kandhai et al., 1998; Fredrich et al., 1999). Another advantage of the LB method is that the implementation is very simple, and portable for different computer platforms. It is also ideal for parallel implementation, since most operations in the LB method are local. Lastly, it may be easier to incorporate more mesoscopic physics, such as mass transfer, chemical reaction and diagenesis, in the LB method than in the Navier-Stokes equations themselves, since the lattice Boltzmann equation is closely related to the continuum Boltzmann equation of nonequilibrium statistical mechanics (Succi, 2001). For certain applications, such as multiphase flow in porous media, there is a growing consensus that the LB method is a strong contender for the best fluid-simulation approach currently available (Fredrich et al., 1999; Succi, 2001). Details on algorithm and implementation can be found in Ladd (1994) and Keehm (2003).

Recent advances in imaging techniques using X-ray microtomography make it possible to obtain 3D pore structures at high resolution. The digital rock sample used in this study was reconstructed from X-ray images of Fon-

tainebleau sandstone at 7.5μm spatial resolution. A subset of the digital Fontainebleau sandstone is shown in Fig 1(a) with 200×150×150 nodes. The flow simulation is done with an assigned pressure gradient (∇P) across opposite faces of cubes. From the local flux, we calculate a volume-averaged flux $\langle q \rangle$. Then, the macroscopic permeability (κ) is calculated using the following:

$$\langle q \rangle = -\frac{\kappa}{\eta} \nabla P , \tag{1}$$

where η is the dynamic viscosity of the fluid. Fig. 1(b) shows the distribution of local fluid flux after flow simulation on the subset in Fig. 1(a). The predicted permeability from the LB flow simulation shows quite a good match with laboratory measurement in Fig.1(c). Moreover, the LB simulation gives a detailed description of local flow properties, such as local fluid velocity and local fluid pressure. These pieces of information are very useful for complex coupled problems, such as flow-limited diagenesis and chemical reaction with fluid in porous media.

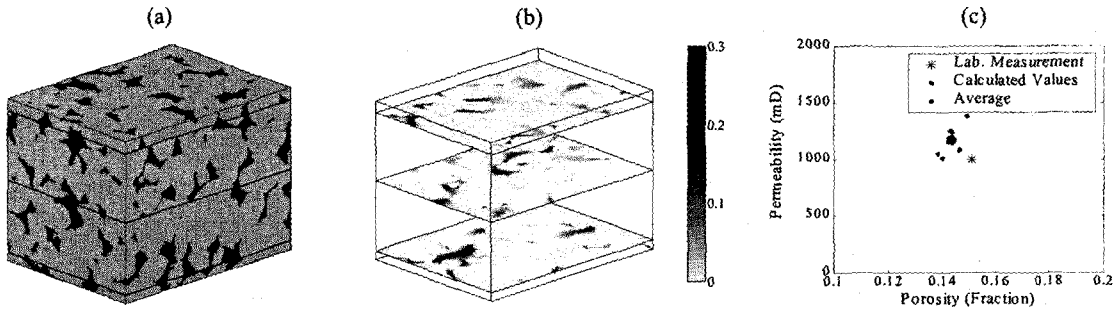

Fig. 1. (a) A subset of 3D pore structure from digital Fontainebleau sandstone with 15% porosity. (b) Local fluid flux from flow simulation at selected cross-sections. The flux values are normalized by the maximal value. (c) Permeability from laboratory measurement and from the LB flow simulations. A star symbol denotes laboratory measurement, blue dots are calculated permeabilities from six subsets, and a red circle is an averaged value.

3. Two-phase Lattice-Boltzmann Flow Simulation

In two-phase flow implementation using the LB method, we follow almost the same procedures as in the single-phase case, except that we have two different types of particles representing two immiscible fluids, and we need to incorporate surface tension and wettability as well as pressure gradient. The two immiscible fluids – non-wetting and wetting fluids, are commonly called red and blue particles respectively, as they were introduced by Rothman and Keller (1988). This concept is roughly equivalent to have color-dyed fluids, which allows us to see the fluid motion but does not affect the fluids themselves. Interactions between these two colors are the key ingredient of two-phase fluid flow. For instance, an immiscible two-phase flow can be simulated with a local interaction between particles with the same type and a local repulsion between particles of different types. For this reason, a color gradient is computed using the color densities of nearest neighboring nodes. The direction of this gradient determines the local interface between two fluids. Then the post collision density distribution of each fluid is chosen so that a particle of a given color preferentially moves in the direction where the same color species reside. Mass and momentum of each type of fluid should be conserved during these procedures. Extensive details can be found in Rothman and Zaleski (1997) and Keehm (2003). Due to the additional calculation, two-phase flow simulation requires very intensive floating-point calculations, one or two order of magnitude higher than single-phase flow simulations. We developed an efficient parallel two-phase LB code (Keehm et al., 2002). Our optimized code runs 12 times faster with 14 processors than its serial counterpart, while the generic parallel code is only 4 times faster. This efficient parallel two-phase flow simulator was used for most two-phase flow calculations in this paper.

Verification of Implementation

In this section, the implementation of the two-phase LB method is applied to many different idealized situations in which the results are already known from theory or laboratory measurements. This will show that the implementation is valid and applicable for real physical two-phase flow in porous media.

A common experiment for capillary pressure between two immiscible fluids is to use spherical bubbles of non-wetting fluid (Gunstensen and Rothman, 1992). In this case, the capillary pressure is given by Laplace's equation (Dullien, 1992),

$$P_{in} - P_{out} = \frac{2\gamma}{R}, \tag{2}$$

where P_{in} and P_{out} are pressures inside and outside of the bubble, γ is the interfacial tension and R is the radius of the bubble. Four different sizes of bubbles (Fig. 2) are used for the numerical experiment. Fig. 2(b) shows the capillary pressures for four different bubbles. The simulated values (dots) are obtained by simply calculating pressures inside and outside after the numerical simulations. The numerical results show very good agreement with the theoretical prediction. Small discrepancies come from the discretization effect of the bubble. This numerical experiment shows that our implementation honors Laplace's equation for capillary pressure.

Fig. 3 shows different wettability situations. Initially, the non-wetting phase is initially located at the bottom-center of the box. With neutral wettability, the contact angle shows 90° as theory predicts. As the wettability increases, the contact angle decreases accordingly, and eventually the non-wetting phase is separated from the bottom and forms a spherical bubble. Therefore the implementation not only replicates the right contact angles but also handles a wide range of wettability. In fact, we can assign different wettability at each node and it is possible to model complex mixed-wet system with our implementation.

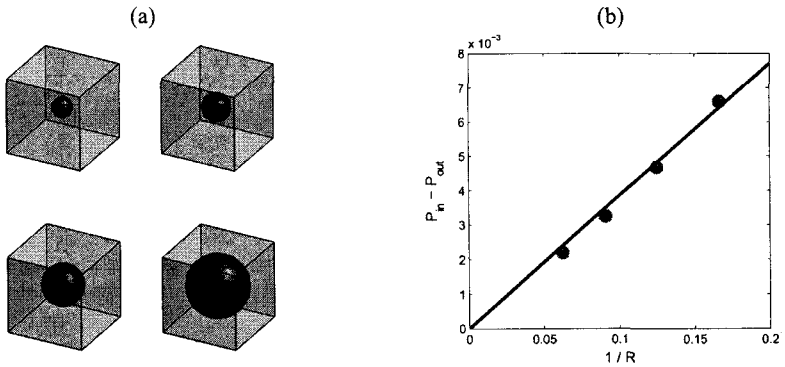

Fig. 2. (a) Four different sizes of non-wetting bubbles in a sea of wetting-phase fluid. (b) Capillary pressure vs. reciprocal of bubble radius. Simulated values (dots) agree well with the theoretical prediction (solid line).

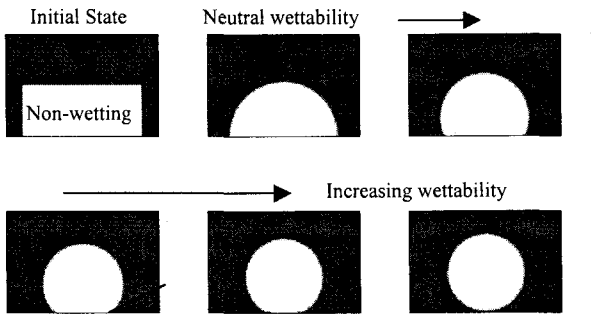

Fig. 3. Contact angles (θ) by the two-phase Lattice-Boltzmann simulation. Each plot is shown as a cross-sectional view. Initially the non-wetting fluid is located at the bottom center of the box. As wettability increases, the contact angle decreases accordingly. Eventually the non-wetting phase is detached from the bottom and forms a spherical bubble.

A well-studied model of immiscible displacement, the so-called pore doublet model, is a good test to verify if the simulation properly models the capillary pressure in a simple but realistic pore structure. A typical pore doublet consists of two tubes with different diameters, joined at both ends (Fig. 4). Since the capillary pressure is inversely proportional to the radius of the tube, the capillary pressure of the smaller tube is greater than that of the bigger tube. Drainage-type snap-off occurs when the external pressure gradient is big enough to overwhelm the capillary pressure of the bigger tube, but is not big enough for the smaller tube. Theory and laboratory experiments show that

under this condition the wetting phase in the smaller tube is trapped while that in the bigger tube is replaced by the non-wetting phase (Chatzis and Dullien, 1983). Fig. 4 shows that the two-phase LB method successfully replicates the drainage-type snap-off, which tells us that the method accurately describes capillary pressure in porous media.

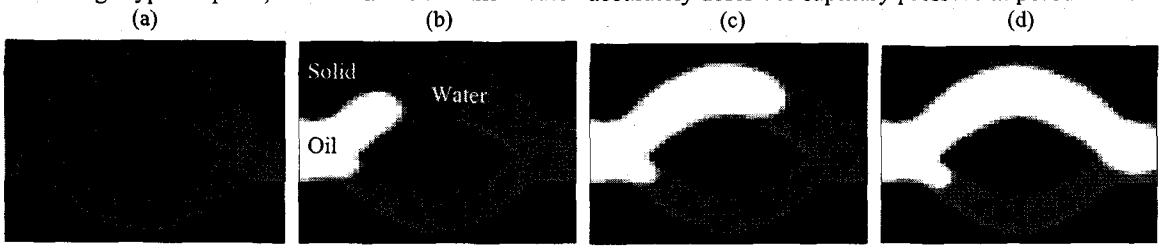

Fig. 4. Drainage-type snap-off in a doublet. (a) Initial stage. Pore space is completely saturated with water (wetting phase). (b) After 5000 iterations. Oil is replacing water in the system. (c) After 10000 iterations. (d) Final stage. There is a continuous oil phase through the bigger pore, while the water phase is trapped in the smaller pore.

Two-phase Flow in Fontainebleau Sandstone

This section presents two-phase flow simulations in realistic and complex porous media. If two fluids were macroscopically separated in porous media, each phase would satisfy Darcy's equation:

$$q_w = -(\frac{\kappa_{rw}\kappa}{\mu_w})\frac{dP_w}{dx},$$
$$q_n = -(\frac{\kappa_{rn}\kappa}{\mu_n})\frac{dP_n}{dx} = -(\frac{\kappa_{rn}\kappa}{\mu_n})\frac{d(P_n - P_c)}{dx}, \quad (3)$$

where the subscripts w and n denote wetting and non-wetting fluids and P_c is the capillary pressure. The new parameters, κ_{rw} and κ_{rn} are called relative permeabilities for the wetting and non-wetting phases, respectively. There are typically two kinds of laboratory measurement techniques for two-phase fluid flow and relative permeability estimation – steady state and unsteady state methods. Both techniques were implemented and simulated, although the numerical implementations are a little different from the laboratory measurement techniques. Details on each laboratory technique can be found in Tiab and Donaldson (1996).

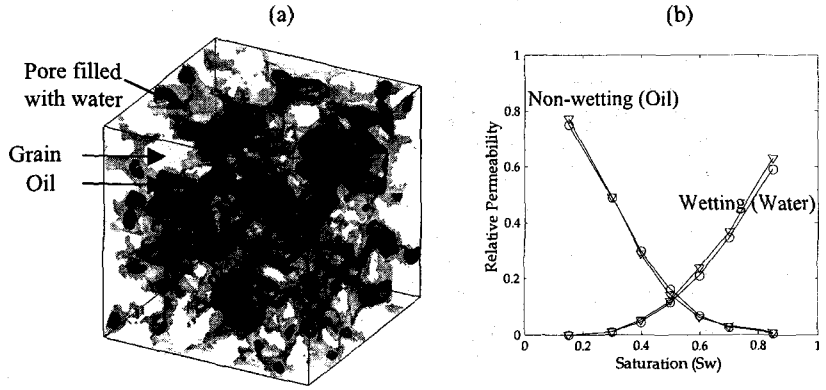

Fig. 5. (a) Distribution of two fluids after the steady-state simulation. White parts denote solid grains and greenish yellow denotes pore structure filled with water. The oil phase is shown in red. Fluid flows from the right-hand side to the left. (b) Relative permeability curves from two different subsets of the digital Fontainebleau sandstone samples.

Fig. 5(a) shows the final distribution of two fluids in the Fontainebleau sandstone sample after the steady-state flow simulation. The solid grains are shown as white. Green geometry is the pore structure filled with water, and red denotes the oil phase. We can see how complexly the two fluids are distributed. The relative permeability curves are obtained from the steady state flow simulation as functions of water (wetting phase) saturation (Sw). Fig. 5(b) shows wetting and non-wetting relative permeability curves. In this calculation, we use a digital rock with 256×256×256 nodes and the typical calculation time is about 2 hours by the parallel simulator with 14 processors, while serial simulator took more than a day on a PC workstation with a 1.7GHz P4 processor.

The unsteady-state simulation technique mimics oil migration and production in oil reservoirs. Initially, the rock sample is fully saturated with water. Oil is pumped into the sample and water is drained until no more water is produced (drainage). The saturation at this point is often called irreducible water saturation. Then the sample is jacketed and allowed to adjust to capillary equilibrium. After achieving equilibrium, water is pumped into the sample (imbibition), and the volumes of the two fluids at the inlet and outlet are measured. Fig. 6 shows snapshots during the simulations. The drainage simulation is shown in the upper row. Initially the sample is completely water-saturated, and then the oil phase replaces water in big and well-connected pores first, and forms finger-type shapes. Finally no more water is produced and the drainage simulation is finished. The oil movement is not very continuous during the drainage. The oil phase gathers in big pores and suddenly moves to neighboring pores through pore throat, i.e. intermittent flow. The irreducible water saturation is about 30%. At the imbibition in Fig. 6(b), we can observe residual oil saturation, which is the volume fraction of trapped oil.

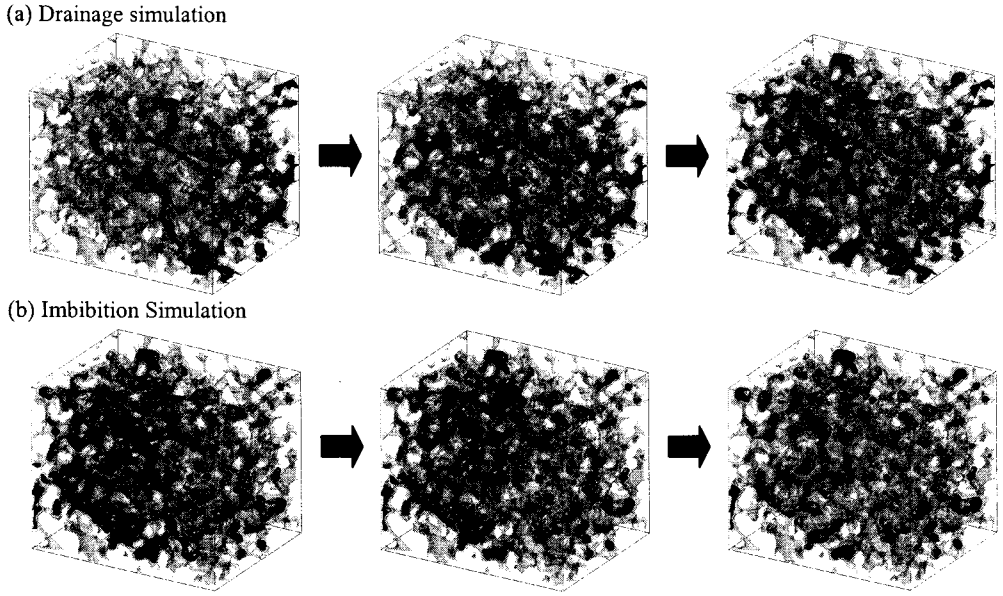

Fig. 6. Two-phase flow in Fontainebleau sandstone. Isosurface plots of snapshots during (a) drainage and (b) imbibition simulations. Color notations are the same as in Fig. 5(a). Pumping fluid is injected from the right-hand side.

We have shown that the two-phase LB method represents realistic two-fluid flow in complex pore geometry reasonably well. Both the steady state and unsteady state simulations can replicate laboratory measurements. Moreover, the LB method can give local parameters at every node, such as pressure, saturation and flux as a function of location and time. These parameters can be used for other applications, such as capillary pressure curve simulation and diagenesis with two-phase fluids. Through the numerical experiments, we found that the implementation of the two-phase LB method can be a good candidate for calculating relative permeability and also for exploring the pore-scale physics of two-phase fluid flow.

4. Applications using the LB Fluid Flow Simulators

This chapter presents two research applications using the single-phase and two-phase LB simulators – permeability estimation from this sections and effect of sweep efficiency by different initial distribution of two fluids. Although the models are rather simple, they give enough insight on pore-scale physics and versatility of pore-scale simulations. Although it is not presented in this paper, the LB simulator was also used for flow-limited diagenesis modeling (Keehm et al., 2001).

Permeability Estimation from Thin Sections

Since permeability is a function of pore geometry only, we can predict permeability exactly with detailed data on pore geometry. However, detailed 3D description is very expensive and not widely available, although recent advances in X-ray microtomography techniques can provide a detailed 3D description of the pore structure (Hazlett,

1995; Coker et al., 1996). Often, pore geometry information is limited to 2D thin sections, thus indirect permeability prediction techniques from thin sections have been widely introduced. Commonly, empirical methods, such as the Kozeny-Carman relation based on simple cylindrical pore geometry, have been widely applied because they are easy to use (Dullien, 1992; Mavko and Nur, 1997). However, they give little insight into the underlying relation between pore geometry and permeability. The models also require other measurements such as the specific surface area and the formation factor which is difficult to measure directly from thin sections (Walsh and Brace, 1984), and often have fitting parameters that need to be calibrated with permeability data (Dullien, 1992). We propose a new method of permeability prediction from thin sections, using flow simulation in stochastically reconstructed 3D porous media. The only required input data in our method are thin section images. The 3D porous media are reconstructed by the sequential indicator simulation (SIS) (Deutsch and Journel, 1998). The reconstruction simulations are performed with statistical parameters (porosity and variogram) from thin sections. Details can be found in Keehm et al. (submitted).

Thin sections were obtained from sandstone samples of the Daqing oil field (Prasad and Nur, submitted). They are relatively clean sandstones with clay content between 4-10%. Porosity and Klinkenberg-corrected air permeability were measured at room pressure and at 5.5 MPa confining pressure under controlled room temperature. The porosity ranges from 20% to 30% and the permeability ranges from 40mD to 1,700mD. Fig. 7(a) shows a scanned image of a thin section sample and the yellow scale bar denotes 1mm. From the scanned image, we performed image processing to create a binary image containing pore and grains. The porosity and variogram were calculated from the binary image and 3D digital pore geometry was reconstructed by SIS. An example of reconstructed porous media is shown in Fig. 7(b). We performed the LB flow simulation in the reconstructed porous media and obtained permeability estimates. Predicted permeabilities from all seven thin sections in Fig. 7(c) show very good agreement with laboratory measurements over a wide range of permeability.

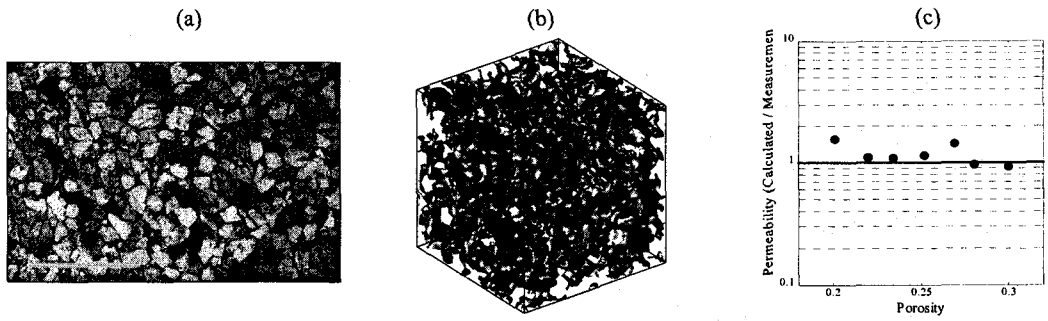

Fig. 7. (a) A scanned image of a thin section sample. (b) Reconstructed 3D pore geometry. (c) Predicted permeability and laboratory measurements. Permeability values are shown as the ratios of calculated permeability to laboratory measurement. The solid line denotes perfect prediction.

Effect of Initial Distribution of Two Fluids

The spatial distribution of pore fluids can have a significant impact on physical properties of rocks. For example, elastic properties of a rock with uniform saturation of fluids may be very different from those with patchy saturation (Sengupta, 2000). Similarly, the original distribution of two fluids in a pore structure will have a significant impact on how the two fluids flow and finally what the relative permeability will be. We investigate the effect of initial two-fluid distribution on the sweep efficiency. Two different initial distributions of fluids are shown in Fig. 8 The upper row shows patchy-type saturation, where the oil phase is located at the center of the sample, while the lower row starts with a final distribution from the drainage simulation. Both have initially about 40% water saturation. As the simulation proceeds, the oil phase is replaced by the water phase. Final distributions of two fluids from both cases show noticeable differences. The residual oil saturation from patchy saturation is larger than from drainage simulation, and the locations of residual oil are also very different. Fig. 9 shows the saturation change during the drainage simulations. The water replaces oil less efficiently in the sample with patchy saturation. The figure also shows the difference in residual oil saturation more clearly. From this simple example, we observed that our implementation can simulate the subtle details of two-fluid distributions in pore geometry realistically, and we showed the potential of two-phase LB implementation for exploring the pore-scale physics of two-phase fluid flow in real rock. Though this model is quite simple, our LB two-phase flow simulator is ready to explore more interest-

ing and complex phenomena with our LB two-phase flow simulator, such as sweep efficiency in mixed-wet systems and diagenesis with two-phase fluid flow.

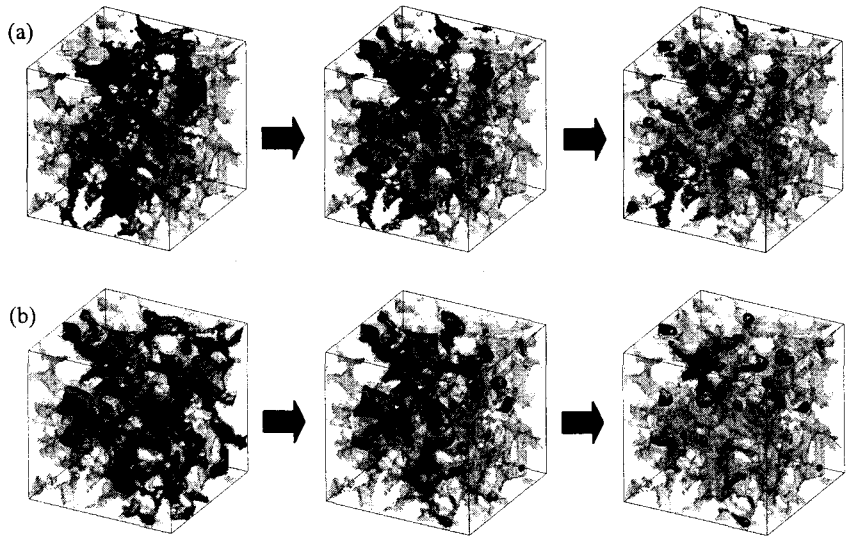

Fig. 8. Imbibition simulations on (a) a sample with patchy saturation, and (b) a sample from a drainage simulation.

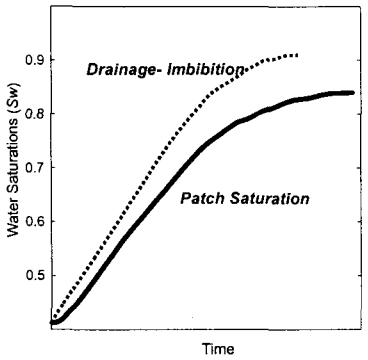

Fig. 9. Saturations curves for sweep efficiency. The two initial conditions come from imbibition simulation and from patchy saturation.

5. Conclusions

We developed and implemented single-phase and two-phase Lattice-Boltzmann (LB) flow simulators. The single-phase flow simulator successfully replicates fluid flow in a digitized sandstone sample, and predicts permeability very accurately. An application using the single-phase flow simulator is also proposed: a permeability estimation technique from thin sections. The LB flow simulation in stochastically reconstructed 3D porous media is a robust combination for permeability prediction from thin sections, providing very good agreement with laboratory measurements over a wide range of permeability. The main strength comes from the fact that the LB simulator rigorously handles stochastically reconstructed microstructures with statistical noises.

We extended the single-phase LB algorithm to two-phase systems, and implemented two-phase LB flow simulator. To overcome the long calculation time of two-phase simulations, parallel two-phase flow simulator was implemented for efficient and accurate calculation. Our optimized parallel code runs 12 times faster with 14 processors than its serial counterpart, while the generic parallel code is only 4 times faster. With this efficient parallel two-phase flow simulator, we verified that the implementation replicates realistic two-phase flow in porous media by various numerical experiments. The LB two-phase simulator successfully calculated relative permeability of a

digital Fontainebleau sandstone model. It is also ready for a wide range of applications, including the effect of wettability, capillary pressure and hysteresis, and relative permeability estimation from thin sections.

The main benefit of the Lattice-Boltzmann flow simulation is to use the real structures of porous media, which will give a unified framework (computational rock physics framework) by combining other pore-scale simulation techniques, such as simulators for acoustic/elastic properties, electrical conductivity and NMR response. These rigorous pore-scale simulators can significantly complement the physical laboratory, with several distinct advantages: (1) rigorous prediction of the physical properties, (2) interrelations among the different rock properties in a given pore geometry, and (3) simulation of dynamic problems, which describe coupled, nonlinear, transient and complex behavior of earth systems.

References

Chatzis, I., Dullien, F. A. L., 1983, Dynamic immiscible displacement mechanisms in pore doublets: Theory versus experiment, J. Colloid Interface Sci., 91, 199–222.

Chen, S., Wang, C., Shan, X., Doolen, G. D., 1992, Lattice Boltzmann computational fluid dynamics in three dimensions, J. Stat. Phys., 68, 379–400.

Chopard, B., Droz, M., 1998, Cellular automata modeling of physical system, Cambridge Univ. Press.

Coker, D. A., Torquato, S., Dunsmoir, J. H., 1996, Morphology and physical properties of Frontainebleau sandstone via tomographic analysis, J. Geophy. Res., 101, 497–506.

Deutsch, C. V., Journel, A. G., 1998, GSLIB: Geostatical software library and user's guide, Oxford Univ. Press.

Doolen, G. D. (Editor), 1990, Lattice gas methods for partial differential equations, Addison-Wesley.

Dullien, F. A. L., 1992, Porous media: Fluid transport and pore structure, Academic Press.

Fredrich, J. T., Noble, D. R., O'Connor, R. M., Lindquist, W. B., 1999, Development, Implementation, and Experimental Validation of the Lattice-Boltzmann Method for Modeling Three-dimensional Complex Flows, Sandia National Laboratory report SAND99-0369, Sandia National Laboratory, Sandia.

Gunstensen, A. K., Rothman D. H., 1992, Microscopic modeling of immiscible fluids in three dimensional by a Lattice Boltzmann method, Europhys. Lett., 18, 157–161.

Hazlett, R. D., 1995, Simulation of capillary dominated displacements in microtomographic images of reservoir rocks, Transport in Porous Media, 20, 21–35.

Kandhai, D., Vidal, D. J.-E., Hoekstra, A. G.,Hoefsloot, H., Iedema, P., Sloot, P. M. A., 1998, A comparison between lattice-Boltzmann and finite-element simulations of fluid flow in static mixer reactors, Int. J. Modern Phys. 9, 1123-1128.

Keehm, Y., 2003, Computational rock physics: Transport properties in porous media and applications, Ph.D. Dissertation, Stanford University, Stanford.

Keehm, Y., Mukerji, T., Nur. A., 2001, Computational rock physics at the pore scale: Transport properties and diagenesis in realistic pore geometries, The Leading Edge, 20, 180–183.

Keehm, Y., Mukerji, T., Nur, A., 2002, Efficient parallel implementation of two-phase lattice-Boltzmann flow simulation, Expanded Abstract in 72nd Ann. Mtg., Soc. Expl. Geophys., Salt Lake City, UT.

Keehm, Y., Mukerji, T., Nur. A., Submitted to Geophy. Res. Lett., Permeability estimation from thin sections: 3D reconstruction and lattice-Boltzmann flow simulation.

Ladd, A. J. H., 1994, Numerical simulation of particulate suspensions via s discretized Boltzmann equation. Part 1. Theoretical foundation, J. Fluid Mech., 271, 285–309.

Martys, N. S., Chen, H., 1996, Simulation of multicomponent fluids in complex three-dimensional geometries by the lattice Boltzmann method, Phys. Rev. E, 53, 743–750.

Mavko, G., Nur, A., 1997, The effect of a percolation threshold in the Kozeny-Carman relation, Geophysics, 62, 1480–1482.

Prasad, M., Nur, A., submitted to Geophysics, Acoustic and depositional properties of fluviatile sandstones.

Rothman, D. H., Keller, J. M., 1988, Immiscible cellular-automata fluids, J. Stat. Phys., 52, 1119–1127.

Rothman D. H., Zalesky, S., 1997, Lattice-gas cellular automata, Cambridage Univ. Press.

Sengupta, M., 2000, Integrating rock physics and flow simulation to reduce uncertainties in seismic reservoir monitoring, Ph.D. Dissertation, Stanford University, Stanford.

Succi, S., 2001, The Lattice Boltzmann equation for fluid dynamics and beyond, Oxford Univ. Press.

Tiab, D., Donaldson, E., 1996, Petrophysics: Theory and practice of measuring reservoir rock and transport properties, Gulf Publishing Company.

Walsh, J. B., Brace, W. F., 1984, The effect of pressure on porosity and transport properties of rock, J. Geophy. Res., 89, 9425–9431.